

THE PHASES DIFFERENTIAL ASTROMETRY DATA ARCHIVE. III. LIMITS TO TERTIARY COMPANIONS

MATTHEW W. MUTERSPAUGH^{1, 2}, BENJAMIN F. LANE³, S. R. KULKARNI⁴, MACIEJ KONACKI^{5, 6}, BERNARD F. BURKE⁷,
M. M. COLAVITA⁸, M. SHAO⁸

Draft version May 22, 2022

ABSTRACT

The Palomar High-precision Astrometric Search for Exoplanet Systems (PHASES) monitored 51 subarcsecond binary systems to evaluate whether tertiary companions as small as Jovian planets orbited either the primary or secondary stars, perturbing their otherwise smooth Keplerian motions. Twenty-one of those systems were observed 10 or more times and show no evidence of additional companions. A new algorithm is presented for identifying astrometric companions and establishing the (companion mass)-(orbital period) combinations that can be excluded from existence with high confidence based on the PHASES observations, and the regions of mass-period phase space being excluded are presented for 21 PHASES binaries.

Subject headings: astrometry – binaries:close – binaries:visual – techniques:interferometric

1. INTRODUCTION

Searches for planets in close binary systems explore the degree to which stellar multiplicity inhibits or promotes planet formation. The orbits in which planets in binary systems can be stable are divided into three classes: (1) P-type (for “Planetary Type”), or circumbinary planets, which orbit both stars at a separation much larger than that of the stars themselves, (2) S-type (for “Satellite Type”) which orbit either the primary or the secondary star but not both, with an orbital size much smaller than the distance between the stars, and (3) L-type, for planets found at Lagrangian points (Dvorak 1982). The Palomar High-Precision Astrometric Search for Exoplanet Systems (PHASES) was a search at the Palomar Testbed Interferometer (PTI; Colavita et al. 1999) targeting 51 close binaries (semimajor axis a few 100 milliarseconds) to identify S-type planetary companions to either star in each pair by measuring the relative separations of the stars with $\sim 35\mu\text{as}$ astrometric precisions (Lane & Muterspaugh 2004).

Current theory is that planets form in and from material of dusty disks observed around young stars. Some models in which giant planet formation occurs over large amounts of time (e.g., the core-accretion scenario at 1-10 Myr) predict that an extra-turbulent environment,

such as those around binary stars, will disrupt planet formation by dispersing the protoplanetary disk while it is young or increasing impact speeds between planetesimals preventing accretion into larger objects (Marzari & Scholl 2000; Marzari et al. 2007). If the timescale is short (as in the gravitational instability theory), the process can happen before the disk is disrupted, or even be enhanced due to additional instabilities in the planet forming disks (Boss 1998).

The leading theories have helped promote a common belief that planet formation is difficult or inhibited in binary or multiple stars because these disks might be more short-lived. However, a lower limit of 22% of known planet hosting stars have distant stellar companions (Raghavan et al. 2006). Given that multiplicity is the norm in the solar neighborhood (57%; Duquennoy & Mayor 1991) and star-forming regions (Simon et al. 1995), the entire issue of planets in binary and multiple stars cannot be ignored if a complete census of planets is to be taken. Indeed, searching for planets in such systems acts as a test of planet formation models in complex dynamical environments (see, for example, Desidera & Barbieri 2007).

While planets in binaries appear to be common, most of the binaries being surveyed have very wide separations and the companion star has little gravitational influence on the environment of the planet host. PHASES was different in that the stellar companions were much closer to the planet-hosting star—only a handful of binaries targeted by other programs have these small physical separations. These systems place much stronger constraints on the impact of dynamics on planet formation.

Studying relatively close pairs of stars, where dynamic perturbations are the strongest, provides the most restrictive constraints of this type (see, for example, Thébaud et al. 2004). Searching for planets in those systems can determine whether the planet formation mechanisms found in nature are sensitive to binary dynamics or not, a property which must be matched by theoretical models (Hatzes & Wuchterl 2005). It may be that multiple mechanisms contribute to giant planet formation in nature. Establishing the rate at which giant planets exist in binaries will distinguish the relative frequencies at

matthew1@coe.tsuniv.edu, blane@draper.com, maciej@ncac.torun.pl

¹ Department of Mathematics and Physics, College of Arts and Sciences, Tennessee State University, Boswell Science Hall, Nashville, TN 37209

² Tennessee State University, Center of Excellence in Information Systems, 3500 John A. Merritt Blvd., Box No. 9501, Nashville, TN 37209-1561

³ Draper Laboratory, 555 Technology Square, Cambridge, MA 02139-3563

⁴ Division of Physics, Mathematics and Astronomy, 105-24, California Institute of Technology, Pasadena, CA 91125

⁵ Nicolaus Copernicus Astronomical Center, Polish Academy of Sciences, Rabińska 8, 87-100 Torun, Poland

⁶ Astronomical Observatory, Adam Mickiewicz University, ul. Słoneczna 36, 60-286 Poznan, Poland

⁷ MIT Kavli Institute for Astrophysics and Space Research, MIT Department of Physics, 70 Vassar Street, Cambridge, MA 02139

⁸ Jet Propulsion Laboratory, California Institute of Technology, 4800 Oak Grove Dr., Pasadena, CA 91109

Table 1
Close Binaries with Planets.

Object	a (AU)	e^a	M_1/M_2^b	R_t (AU) ^c	References
HD 188753 ^d	12.3	0.50	1.06/1.63	1.3	1, 2, 3
γ Cephei	18.5	0.36	1.59/0.34	3.6	4, 5
GJ 86 ^e	~ 20	...	0.7/1.0	~ 5	6, 7, 8
HD 41004 ^f	~ 20	...	0.7/0.4	~ 6	9
HD 126614	~ 45	...	1.145/0.324	~ 15	10
HD 196885	~ 25	...	1.3/0.6	~ 8	11

References. — (1) Konacki 2005; (2) Eggenberger et al. 2007; (3) Mazeh et al. 2009; (4) Campbell et al. 1988; (5) Hatzes et al. 2003; (6) Queloz et al. 2000; (7) Mugrauer & Neuhäuser 2005; (8) Lagrange et al. 2006; (9) Zucker et al. 2004; (10) Howard et al. 2010 (11) Chauvin et al. 2006

^a When the eccentricity is unknown, the projected binary separation is used as an approximation, except in the case of HD 126614, where a linear velocity trend due to the star is observed, and the binary itself has been resolved, leading to two possible solutions with $a = 40^{+7}_{-4}$ and 50^{+2}_{-3} AU.

^b Mass of star hosting planet divided by mass of the companion star.

^c The distance from the primary star at which a disk would be rapidly truncated by tides (Pichardo et al. 2005).

^d The companion star itself is a binary with the semimajor axis 0.67 AU. This candidate is controversial due to minimal data in the discovery paper with sporadic observing cadence and a lack of evidence found by Eggenberger et al. (2007) and Mazeh et al. (2009).

^e The companion star is a white dwarf of mass $\simeq 0.5M_{\odot}$. To estimate R_t at the time of formation, an original companion mass of $1M_{\odot}$ is assumed.

^f The secondary also has a substellar companion—a brown dwarf with a 1.3 day period.

which different processes contribute.

It can be shown that dynamic interactions between stars in young clusters can result in close binaries ($a < 50$ AU) having S-type planetary companions that did not form in situ in the close binary, but around a single star, which later interacted with a binary, inserting the planet into the system (Pfahl 2005). The low frequency of these interactions would result in less than 0.1% of such binaries hosting planets were this the only mechanism from which such configurations arise (Pfahl & Muterspaugh 2006). Any planet frequency above this level would indicate that the planet formation process can survive the binary star environment—the number of planets beyond that frequency must have formed in situ.

A few close binaries have been identified hosting giant planets and are listed in Table 1. The 5-6 such systems already identified represent a larger frequency of occurrence than such dynamics could explain. Ongoing efforts to identify such systems will need to concentrate on better identifying the statistics of the total number of close binaries that have been included in surveys in order to better understand the planet frequency statistics. In this paper, the null results for the PHASES effort are reported to quantify the population statistics of this search for comparison with the number of candidates discovered (see Paper V).

This paper is the third in a series analyzing the final results of the PHASES project as of its completion in late 2008. The first paper describes the observing method, sources of measurement uncertainties, limits of observing precisions, derives empirical scaling rules to account for noise sources beyond those predicted by the standard reduction algorithms, and presents the full catalog of astrometric measurements from PHASES (Muterspaugh

et al. 2010d). The second paper combines PHASES astrometry with astrometric measurements made by other methods as well as radial velocity observations (where available) to determine orbital solutions to the binaries' Keplerian motions, determining physical properties such as component masses and system distance when possible (Muterspaugh et al. 2010b). The current paper presents limits on the existence of substellar tertiary companions orbiting either the primary or secondary stars in those systems that are found to be consistent with being simple binaries. Paper IV presents orbital solutions to a known triple star system (63 Gem = HD 58728) and a newly discovered triple system (HR 2896 = HD 60318) (Muterspaugh et al. 2010a). Finally, Paper V presents candidate substellar companions to PHASES binaries as detected by astrometry (Muterspaugh et al. 2010c).

Astrometric measurements were made as part of the PHASES program at PTI, which was located on Palomar Mountain near San Diego, CA. It was developed by the Jet Propulsion Laboratory, California Institute of Technology for NASA, as a testbed for interferometric techniques applicable to the Keck Interferometer and other missions such as the Space Interferometry Mission (SIM). It operated in the J ($1.2\mu\text{m}$), H ($1.6\mu\text{m}$), and K ($2.2\mu\text{m}$) bands, and combined starlight from two out of three available 40-cm apertures. The apertures formed a triangle with one 110 and two 87 meter baselines. PHASES observations began in 2002 continued through 2008 November when PTI ceased routine operations.

2. COMPANION SEARCH ALGORITHM

PHASES differential astrometry measurements are presented in Paper I. This includes corrections to the measurement uncertainties, which are used here.

Muterspaugh et al. (2006b) presented an initial analysis algorithm and preliminary results for the range of mass-period phase space in which tertiary companions can be ruled out for eight binaries. This initial algorithm had some limitations that have since been improved upon. These limitations included the fact that only face-on, circular companion orbits were modeled, the algorithm used a statistical analysis that did not account for how the observing cadence can impact the false alarm rate, and the algorithm was very computationally intensive. An alternative analysis method has been developed for identifying candidate companions and establishing the range of mass-period pairings for hypothetical tertiary companions that can be ruled out by the PHASES observations. While still relatively computationally intensive, the new algorithm is less so and solves the other limitations much more completely.

2.1. Identifying Candidate Objects

Cumming et al. (1999) developed a general method for (1) identifying Keplerian signals, (2) estimating the level of confidence in the signal detection, and (3) evaluating the mass threshold (as a function of orbital period) that can be shown not to exist by a given data set, to some level of confidence. This algorithm has been modified for use with the PHASES measurements. The major differences arise from PHASES being astrometric measurements (whereas Cumming et al. (1999) analyzed velocity measurements), the PHASES measure-

ments were two-dimensional in nature, and because the stars are binary and in orbit around each other some degree of model-fitting is necessary even in the case that additional companions are not found. In other words, the no-companion model is not a constant value, but rather the orbit of the binary itself. The model with an additional companion is the binary orbit plus the companion orbit. When evaluating the model that includes an additional companion, it is also crucial to reoptimize the parameters associated with the binary orbit itself, to adjust for the addition of the perturbation orbit. In other words, it is not enough to fit a companion model to residuals that were computed by subtracting an optimized binary model from the original measurements—both components of the model need to be reoptimized. These modifications to the work of Cumming et al. (1999), and the code base for it, were designed, developed, and tested by the first author’s (M.W.M.) team during the SIM Double Blind Test (Traub et al. 2009, 2010), and were demonstrated as reliable during that time.

First, a single Keplerian orbital model was fit to the PHASES data for each star, and the parameters of that orbit were optimized to minimize the χ^2 goodness-of-fit metric. These served as comparison models against which to compare how well the data were represented by alternative models, such as those with the Keplerian plus a perturbation caused by the reflex motion of one star as an additional object orbits it. The best fit χ^2 of the Keplerian orbital model is χ_2^2 , where the 2 subscript indicates only two objects are in the system (the stars of the binary itself).

Second, a double Keplerian orbital model was fit to the data at several possible values of the companion orbital period. During this fitting, all parameters of the known binary orbit were reoptimized (being seeded at their values from the best-fit single Keplerian model to initiate the fitting), as well as the orbital elements of the perturbation model, excluding eccentricity (which was set to zero), time of periastron passage T_o (because it would be degenerate with the Campbell parameter ω when the eccentricity is zero), and orbital period (which was fixed at its seed value, as described below). Thus, while the binary orbit was a full Keplerian model, the perturbation model was circular only, though at any inclination and orientation on the sky. However, in practice the circular orbit model correctly identified most companions having eccentric orbits as well. The orbital model was optimized in the Thiele-Innes parameter set rather than the normal Campbell parameter set to improve computational efficiency (for a recent review, see Wright & Howard 2009). A downhill search algorithm was used to minimize χ^2 of the model in a variant of the standard Levinberg-Marquart approach.

The companion orbital periods at which the double Keplerian model was evaluated were selected in a method inspired by Nyquist frequency sampling. For a data set spanning time T , the set of periods selected was given by $P = 2fT/k$, where k is a positive integer, and f is an oversampling factor. If the times of the data measurements were uniform, $f = 1$ could be safely assumed; however, this is not the case for real measurements. Thus, $f = 3$ was chosen as the oversampling factor in the present analysis to ensure sampling density did not cause

potential companions to be missed. The largest value of k was chosen to be that for which $P = 6$ days, both for computational efficiency, and because astrometry is unlikely to find many objects at shorter orbital periods that are not already known from radial velocity measurements. It was important to examine periods this short to explore effects at the \sim week cadence common for the PHASES observations. Finally, because some orbital curvature could be observed for massive companions with orbital periods longer than the data span T , one additional value of $k = 1/2$ was also evaluated (making the longest period evaluated $P = 2fT/k = 12T$).

At each value of the perturbation orbit’s period, the best-fitting model’s value of χ_3^2 is evaluated (here, the subscript 3 indicates the model represents three objects are in the system). These were used to create a periodogram similar to those in Cumming et al. (1999), for which the largest peak corresponds to the value that best improved the fit to the data. The periodogram values were calculated as

$$z(P) = \left(\frac{2N - 11}{11 - 7} \right) \left(\frac{\chi_2^2 - \chi_3^2(P)}{\chi_3^2(P_{\text{best}})} \right) \quad (1)$$

where N is the number of two-dimensional astrometric measurements (thus, $2N$ total measurements were analyzed), 11 is the number of free parameters in the double Keplerian model (the normal seven Keplerian parameters for the binary orbit, and only four for the perturbation orbit were free parameters, since the epoch of periastron passage T_o , the eccentricity $e = 0$, and orbital period P were held fixed during model fitting), 7 is the number of free parameters in the single Keplerian model, and $\chi_3^2(P_{\text{best}})$ is the overall best (smallest) value of χ_3^2 of all the periods sampled. This statistic follows the F distribution as a test of whether the addition of the second orbit is valid (see, for example, Bevington & Robinson 2003).

2.2. False Alarm Probability of Companion Detection

Because sampling cadence can have effects on the periodogram that are not straightforward to calculate, the false alarm probability (FAP) of a given value of z was calculated by creating synthetic data sets with identical cadence and scatter in the data, rather than directly from the expected F distribution. Cumming et al. (1999) identify two ways of creating synthetic data sets, and note that in practice, the two approaches produce very similar results. One approach is to scramble residuals from the actual measurements, rescaling their values by the ratio of the uncertainties of the replacement measurement and the one actually made at the given time. This has the advantage that the synthetic data set has similar statistical properties to the actual data and does not assume Gaussian (or other) statistics to the data. The alternative is to create synthetic data sets from a random number generator, scaling the random numbers by the measurement uncertainty of a given measurement. The first approach was made more difficult for the PHASES measurements, given their two-dimensional nature, variable measurement uncertainties, variable orientations of the error ellipses on the sky, and the presence of the motion of the binary as a whole. Thus, for the present analysis, the latter approach was selected. A random

number generator created a list of Gaussian-distributed random numbers. The use of Gaussian statistics for the synthetic noise was justified by the distribution of the residuals from PHASES measurements, as demonstrated in Paper I. For each measurement, two random numbers were used to create synthetic data in the basis of the measurement's uncertainty ellipse minor and major axis (in this basis, the two-dimensional uncertainties have zero covariance) and those values are then rotated into the right ascension-declination basis in accordance with the uncertainty covariance. The best-fit single-Keplerian signal was then added to the random values, creating a complete synthetic data set representing the binary motion, but no additional real perturbations. The synthetic data set was analyzed in the same manner as the real data set, and the maximum value of z for that synthetic data was recorded. The process was repeated 1000 times, each time creating a new synthetic data set. The fraction of synthetic data sets producing maximum values of z greater than that observed in the actual data determines the level of confidence, or FAP, that the peak in the data periodogram represents a perturbation created by a real object, rather than being a statistical fluctuation. The value of z of the tenth largest maximum values of z from the synthetic data identifies the level at which a detected signal would have an FAP of $10/1000 = 1\%$.

2.3. Detection Limits

After computing the periodogram and the FAP of its values, the tertiary companion masses which can be shown *not* to exist with high confidence were evaluated, as a function of the orbital period of the tertiary companion. This represents the sensitivity limits of the PHASES survey. For each orbital period P for a potential perturber, 1000 synthetic data sets were produced as above, but both the binary plus an additional Keplerian signal were added to the data set representing a tertiary companion to the system. The parameters describing the second Keplerian were selected in the Campbell set as follows.

- the orbital period P was given by the tertiary companion orbital period being evaluated,
- the epoch of periastron passage T_o was selected from a flat distribution centered at the average time of observation, and covering a span equal to the orbital period P (this range covers all possible non-degenerate values of T_o),
- the eccentricity was selected from a flat distribution between $0 \leq e \leq 0.5$; in practice, the results were fairly accurate for any value of eccentricity,
- the inclination was selected from a flat distribution in $\sin i$,
- ω was selected from a flat distribution between $0^\circ \leq \omega \leq 360^\circ$,
- Ω was selected from a flat distribution between $0^\circ \leq \Omega \leq 360^\circ$, and
- the semi-major axis a was given an initial value close to the average minor axis uncertainty of the

PHASES measurements, though this will be modified upon iteration, as described below.

For the elements that are chosen randomly (T_o , e , i , ω , and Ω), different values were selected for each of the 1000 synthetic data sets being created. Each of the 1000 synthetic data sets were fit to the double Keplerian model; the fit was seeded with the known orbital parameters (with the exception of the perturbing orbit's eccentricity, which was fixed at zero regardless of the actual eccentricity used to generate the synthetic data for equality with the actual search algorithm on real data). During fitting, all seven parameters of the binary orbit were free parameters, as well as i , ω , Ω , and a of the tertiary companion orbit. Also, the best-fit single Keplerian model for the synthetic data set was computed, for use in evaluating z , as

$$z(P) = \left(\frac{2N - 11}{11 - 7} \right) \left(\frac{\chi_2^2 - \chi_3^2(P)}{\chi_3^2(P)} \right) \quad (2)$$

where $\chi_3^2(P_{\text{best}})$ was replaced by χ_3^2 in the denominator, since only one orbital period was being evaluated. The fraction of synthetic data sets with z exceeding the maximum value of z in the actual data (of all orbital periods evaluated) was computed. If the fraction was larger than some specified confidence level (here, 99%), the semimajor axis of the perturbing orbit was decreased for the next iteration; if it was smaller, the semimajor axis was increased. This procedure was iterated, each time generating 1000 new synthetic data sets, until the semimajor axis that creates synthetic data sets for which 99% were found to have z exceeding that of the data was bounded. Once bounded, further iterations refined this bound until the correct semimajor axis was determined to a precision of $4 \mu\text{s}$ or better (corresponding to roughly 1/10 the typical minor axis uncertainty of PHASES measurements). The resulting limiting semimajor axis was converted into the corresponding companion mass necessary to create a reflex motion of one of the stars in the binary by that amount, given the star's mass, the tertiary companion orbital period, and the overall distance to the star system.

2.4. Stability of Orbits

Finally, there is the question of whether the orbits are stable, since the presence of the second star creates a different dynamical environment. Indeed, this is part of the motivation for searching for planets in binaries separated by only 10-50 AU: whether the formation mechanism for giant planets can survive such a dynamic environment. System stability offers an external check for whether a candidate companion is a false identification. The empirical stability rules identified by Holman & Wiegert (1999) are calculated for each binary and set as approximate limits for the ranges over which companions might be expected to have stable orbits using the following relationship:

$$a_c = (0.464 - 0.380\mu - 0.631e + 0.586\mu e + 0.150e^2 - 0.198\mu e^2) a_b \quad (3)$$

where a_c is the semimajor axis of the largest stable orbit, a_b is the semimajor axis of the binary, e is the eccentricity of the binary, and $\mu = m_2/(m_1 + m_2)$ is the mass ratio of the binary, where m_2 is the perturbing star and m_1 hosts

Table 2
Maximum Stable Orbital Periods and Star Masses and Distances Used To Compute Limits

HD Number	$P_{1, \max}$	$P_{2, \max}$	$M_{\text{star}} (M_{\odot})$	$d_{\text{star}} (\text{pc})$
5286	6354	6354	1.00	38.92
6811	16804	16804	3.55	225.73
17904	170	170	2.06	72.10
26690	284	231	0.82	36.48
44926	32410	32410	6.00	438.60
76943	1284	1124	1.04	16.26
77327	591	591	5.20	129.70
81858	2450	1663	1.10	36.36
114378	552	552	1.22	17.89
114378	555	544	1.22	17.89
129246	N/A	N/A	66.00	55.34
137107	1738	1646	1.10	18.50
137391	155	155	1.62	36.10
137909	197	181	1.33	34.12
140159	1357	1357	1.86	57.80
140436	2087	2087	1.86	43.29
155103	149	149	1.66	55.56
187362	87	87	2.35	100.10
202275	148	148	1.19	18.38
202275	157	153	1.19	18.38
202444	2221	2221	1.31	20.37
207652	1209	1209	1.32	33.78
214850	130	133	1.07	34.43

Note. — The maximum stable orbital periods for tertiary companions to the 21 binaries under consideration, and the values of stellar masses and system distances from the Sun used to convert astrometric perturbation amplitude to companion mass. Column 1 is the binary’s HD number. Columns 2 and 3 are the maximum stable orbital periods in days for S-type planets, calculated according to the formula by Holman & Wiegert (1999). Columns 4 and 5 are the stellar mass and distance to the system, respectively; when only visual orbits were available, the mass used is that of the average component, whereas for systems having radial velocity measurements, the lower mass component is assumed, except in the case of HD 81858, for which the mass ratio has large uncertainty and the average component mass is used. Two entries are present for HD 114378 and HD 202275; these systems were specifically modeled by Holman & Wiegert (1999). The first entry lists the maximum stable orbital periods according to their formula, whereas the second entry lists the actual value they list in their Table 4.

the tertiary companion. The limiting orbital periods are listed in Table 2.

3. COMPANION LIMITS FOR SPECIFIC SYSTEMS

In this section, the mass-period pairings for tertiary companions that can be ruled out for each of the 21 binaries are presented. In Figures 1–25, regions shaded gray indicate companion orbital periods that are not expected to be dynamically stable.

3.1. HD 5286

HD 5286 (36 And, HR 258, HIP 4288, WDS 00550+2338) is a pair of subgiant stars with spectral types G6 and K6. The FAP of the highest peak ($z = 5.19$ at $P = 10.1$ days) in the z-periodogram is 23.0%. The 99% confidence level would have been at $z = 8.68$. Figure 1 shows the periodogram and region of mass-period space in which companions can be ruled out with 99% confidence.

3.2. HD 6811

HD 6811 (ϕ And, 42 And, HR 335, HIP 5434, WDS 01095+4715) is a pair of massive, distant B stars (B6IV

and B9V). As a result, astrometry has more limited sensitivity to tertiary companions. The FAP of the highest peak ($z = 4.40$ at $P = 10.4$ days) in the z-periodogram is 47.2%. The 99% confidence level would have been $z = 9.40$. The periodogram and limits to tertiary companions are plotted in Figure 2.

3.3. HD 17904

The periodogram and limits to tertiary companions to HD 17904 (20 Per, HR 855, HIP 13490, WDS 02537+3820) are plotted in Figure 3. The 1269 day subsystem suggested by Abt & Levy (1976) is not seen, nor would it be predicted to be stable if it did exist. This is consistent with the radial velocity studies by Scarfe & Fekel (1978) and Morbey & Griffin (1987) who also found no evidence of such a subsystem. The FAP of the highest peak ($z = 4.87$ at $P = 39.4$ days) in the z-periodogram is 46.2% and $z = 9.10$ would be necessary to reach the 99% confidence level.

3.4. HD 26690

HD 26690 (46 Tau, HR 1309, HIP 19719, WDS 04136+0743) is a single-lined spectroscopic binary with stellar components having masses near that of the Sun. The z-periodogram and mass-period space limits to tertiary companions using just the PHASES observations are presented in Figure 4. The FAP of the highest peak ($z = 9.83$ at $P = 6.34$ days) in the z-periodogram is 2.8%, with 99% confidence at the $z = 11.09$ level. Because the FAP is low, the search was re-evaluated using both the PHASES measurements as well as those from the *Washington Double Star Catalog* (WDS, see references therein Mason et al. 2001, 2010) as evaluated in Paper II. Though lower precision, these measurements have better time coverage and thus help to avoid confusion with the motion of the binary itself. The same set of companion orbital periods was selected for evaluation as for the PHASES-only search, since only the PHASES data are well-suited to identifying tertiary companions. The synthetic data sets generated included synthetic measurements for the non-PHASES data as well; in these cases, Gaussian random values were selected in separation and position angle, with variances equal to the measurement uncertainties in the real data. In this refined search, the highest peak has a value of only $z = 3.28$ (at $P = 6.31$ days), with an FAP of 67.1% and 99% confidence at $z = 7.08$. Thus, it appears that the initial search did not identify a real companion. The resulting z-periodogram and mass-period companion limits are presented in Figure 5.

3.5. HD 44926

HD 44926 (HIP 30569, WDS 06255+2327) is a relatively unstudied binary comprised of a pair of K giants. The orbit and component masses are relatively uncertain, and the values listed here for the masses of companions that can be excluded are equally uncertain. The FAP of the highest peak ($z = 5.49$ at $P = 19.3$ days) in the z-periodogram is 33.5% and 99% confidence would be found at $z = 9.97$. The z-periodogram and mass limits are plotted in Figure 6.

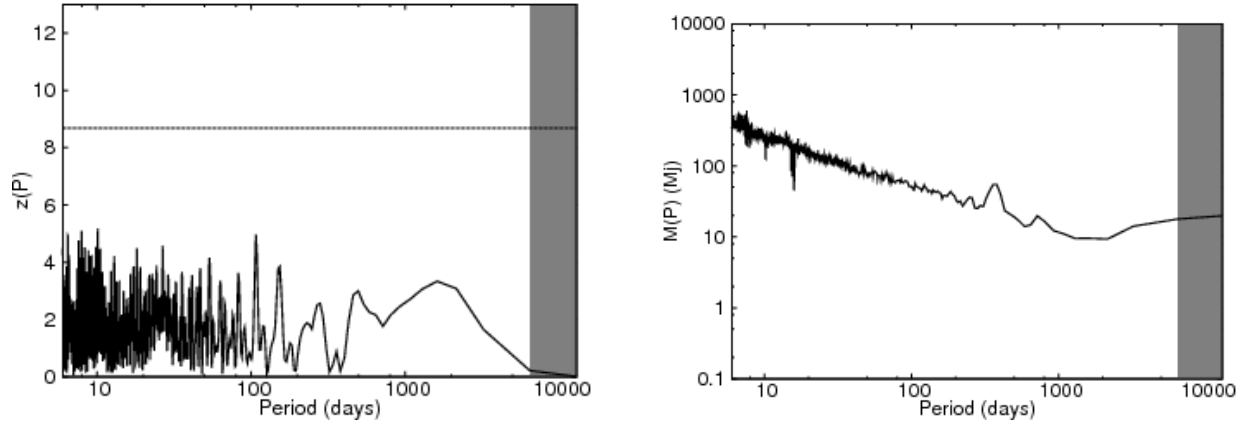


Figure 1. z -periodogram (left) and the mass-period companion phase space for HD 5286 (right). Companions in the regions above the plotted exclusion curve with circular orbits with any orientation are not consistent with the PHASES observations, with 99% confidence. Companions as small as 9.3 Jupiter masses can be ruled out by PHASES observations.

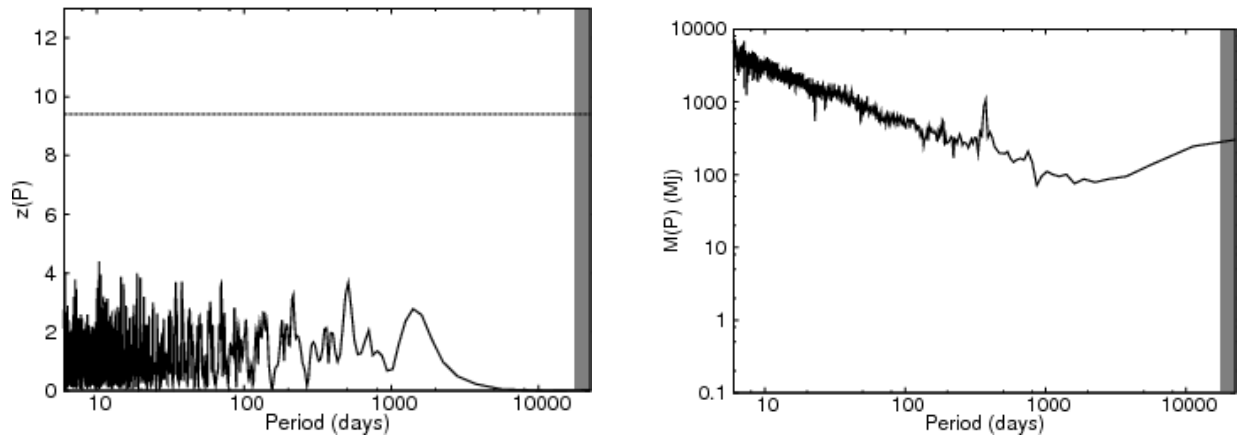


Figure 2. z -periodogram (left) and the mass-period companion phase space for HD 6811 (right). Companions in the regions above the plotted exclusion curve with circular orbits with any orientation are not consistent with the PHASES observations, with 99% confidence. Companions as small as 71 Jupiter masses can be ruled out by PHASES observations.

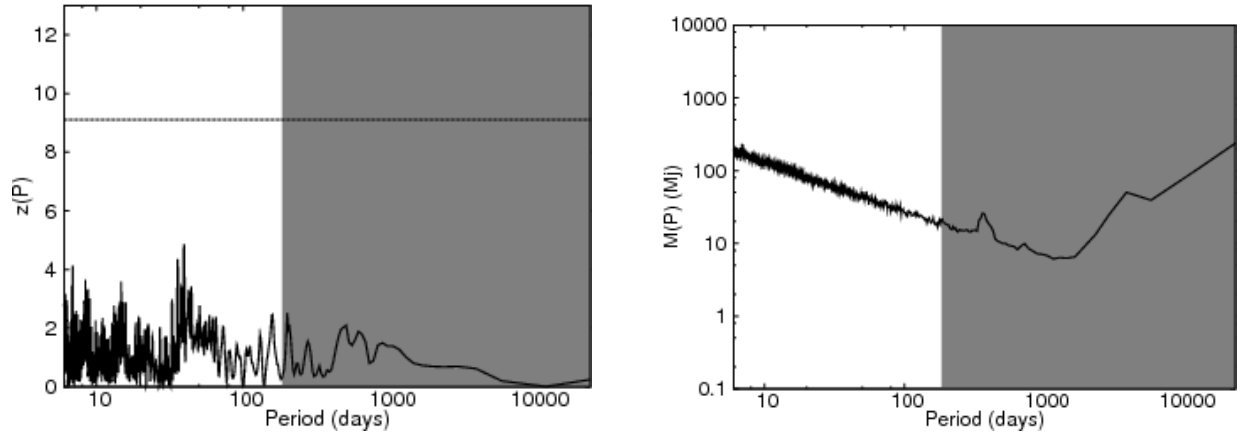


Figure 3. z -periodogram (left) and the mass-period companion phase space for HD 17904 (right). Companions in the regions above the plotted exclusion curve with circular orbits with any orientation are not consistent with the PHASES observations, with 99% confidence. Companions as small as 18 Jupiter masses can be ruled out by PHASES observations.

3.6. HD 76943

HD 76943 (10 UMa—though it is now in the constellation Lynx (Griffin 1999), HR 3579, HIP 44248, WDS 09006+4147) is a relatively nearby double lined spectroscopic binary. The masses and system distance obtained by combining astrometry with velocities from TSU’s AST

in Paper II are not consistent with results from *Hipparcos* or the spectral types. Thus, component masses and distance were used based on the *Hipparcos* results in Söderhjelm (1999). The FAP of the highest peak ($z = 3.78$ at $P = 18.1$ days) in the z -periodogram is 62.9% with 99% detection confidence requiring $z = 10.12$. The periodogram and companion mass limits are plotted in

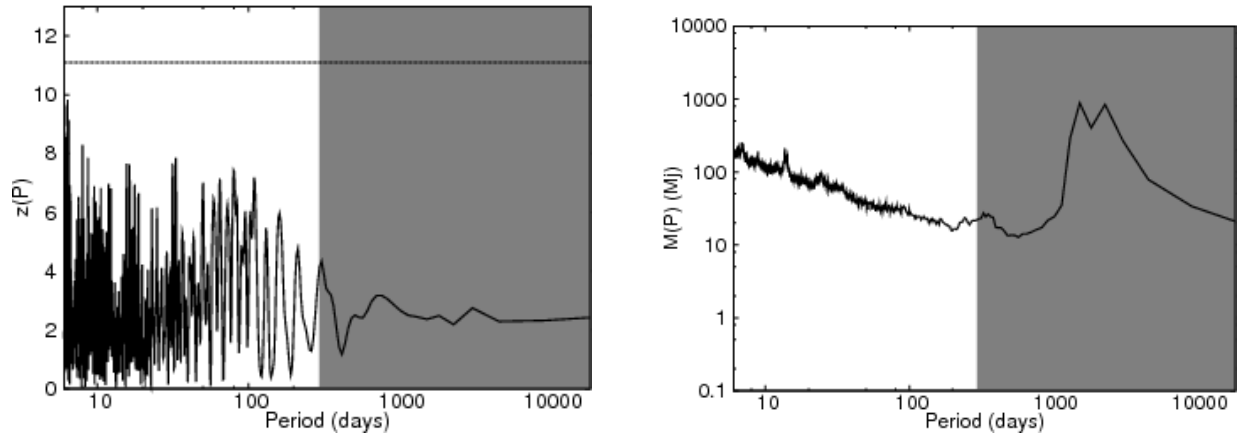


Figure 4. z -periodogram (left) and the mass-period companion phase space for HD 26690 (right). Companions in the regions above the plotted exclusion curve with circular orbits with any orientation are not consistent with the PHASES observations, with 99% confidence. Companions as small as 15.6 Jupiter masses in stable orbits can be ruled out by PHASES observations.

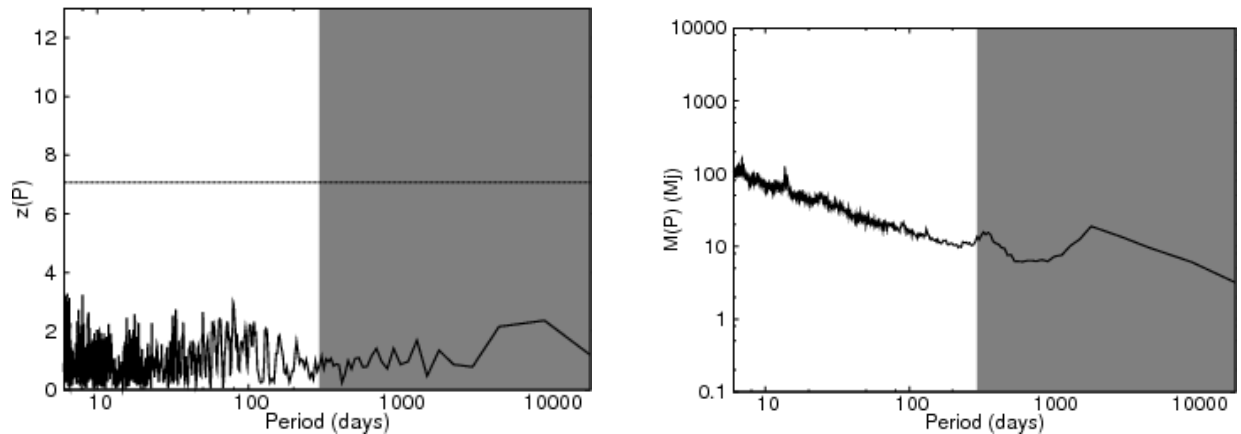


Figure 5. z -periodogram (left) and the mass-period companion phase space for HD 26690 (right). Companions in the regions above the plotted exclusion curve with circular orbits with any orientation are not consistent with the PHASES observations, with 99% confidence. Companions as small as 9.6 Jupiter masses in stable orbits can be ruled out by the combined observations.

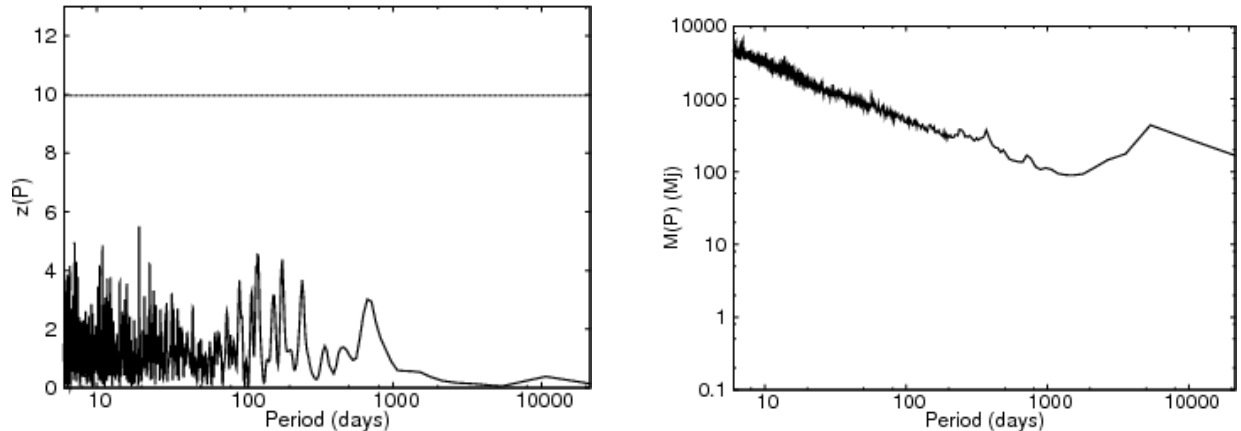


Figure 6. z -periodogram (left) and the mass-period companion phase space for HD 44926 (right). Companions in the regions above the plotted exclusion curve with circular orbits with any orientation are not consistent with the PHASES observations, with 99% confidence. Companions as small as 89 Jupiter masses can be ruled out by PHASES observations.

Figure 7.

3.7. HD 77327

HD 77327 (κ UMa, 12 UMa, HR 3594, HIP 44471, WDS 09036+4709) is a pair of early A dwarf stars. The total mass of the binary is only poorly constrained, so

the values of companion masses ruled out by PHASES astrometry should be interpreted with a similar level of uncertainty. The FAP of the highest peak ($z = 8.94$ at $P = 6.55$ days) in the z -periodogram is 0.3%, and the 99% confidence level for detection is at $z = 8.06$. This low FAP value prompted a second search, this time us-

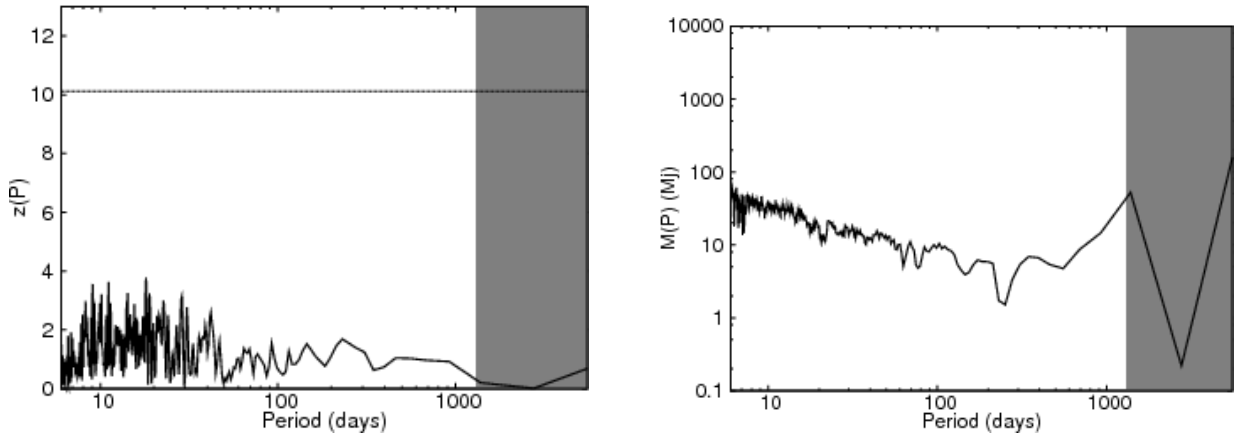


Figure 7. z -periodogram (left) and the mass-period companion phase space for HD 76943 (right). Companions in the regions above the plotted exclusion curve with circular orbits with any orientation are not consistent with the PHASES observations, with 99% confidence. Companions as small as 1.5 Jupiter masses in stable orbits can be ruled out by PHASES observations.

ing both the PHASES and non-PHASES measurements, evaluated at the same perturbation orbital periods as in the PHASES-only search. The addition of non-PHASES measurements helped define the long-term binary orbit, lifting fit degeneracies, and better identifying whether a detected perturbation was due to cadence and the wide orbit, or was evidence of a real companion. The same procedure was used as for HD 26690. The combined search showed a peak value of $z = 3.95$ with an FAP of 44.2% and 99% confidence of detection at $z = 6.57$. Thus, it would appear that this was in fact a spurious detection, despite the low FAP. The z -periodograms and mass limits are plotted in Figures 8 and 9.

3.8. HD 81858

HD 81858 (ω Leo, 2 Leo, HR 3754, HIP 46454, WDS 09285+0903) is a single-lined spectroscopic binary. The mass ratio is only poorly constrained by the available radial velocity data and parallax. Thus, the average component mass of $1.10 M_{\odot}$ was used to convert between astrometric perturbation amplitude and companion mass. The FAP of the highest peak ($z = 4.72$ at $P = 155$ days) in the z -periodogram is 37.8% with 99% detection confidence only for signals with $z > 11.96$. The resulting periodogram and mass-period space limits are presented in Figure 10.

3.9. HD 114378

HD 114378 (α Com, 42 Com, HR 4968, HIP 64241, WDS 13100+1732) is a well studied long period binary. It was included as a specific example system by the tertiary companion stability study of Holman & Wiegert (1999). The FAP of the highest peak ($z = 8.81$ at $P = 6.81$ days) in the z -periodogram is 4.4%, $z = 11.13$ would be required for a reliable detection. The periodogram and companion limits for HD 114378 are plotted in Figure 11.

3.10. HD 129246

HD 129246 (ζ Boo, 30 Boo, HR 5477, HIP 71795, WDS 1411+1344) has an extremely high eccentricity of 0.9977 ± 0.0034 . The distance of closest approach is only 0.3 AU. It is unlikely any companions could have stable orbits in such a system. The binary's eccentricity falls outside the regime examined by Holman & Wiegert

(1999), so it is not surprising their model breaks down in this regime. The binary is useful as a test of the detection algorithm. The FAP of the highest peak ($z = 4.95$ at $P = 8.71$ days) in the z -periodogram is 25.4% with a 1% FAP occurring only for $z > 9.60$. The periodogram and mass limits are plotted in Figure 12.

3.11. HD 137107

HD 137107 (η CrB, 2 CrB, HR 5727, HIP 75312, WDS 15232+3017) is a double-lined spectroscopic binary comprised of stars just slightly more massive than the Sun. It also has a distant (3600 AU), faint, brown dwarf companion in a circumbinary orbit (which has no impact on the astrometric study of the A-B pair; Kirkpatrick et al. 2001). The FAP of the highest peak ($z = 5.66$ at $P = 1323$ days) in the z -periodogram is 19.9% with a 1% FAP occurring only for $z > 8.83$. The periodogram and companion mass limits are plotted in Figure 13.

3.12. HD 137391

The periodogram and mass-period limits for HD 137391 (μ Boo, 51 Boo, HR 5733, HIP 75411, WDS 15245+3723) are plotted in Figure 14. The FAP of the highest peak ($z = 4.65$ at $P = 14.6$ days) in the z -periodogram is 65.1% with 99% detection confidence requiring $z = 10.91$.

3.13. HD 137909

The primary of HD 137909 (“Peculiar Rosette Stone”, β CrB, 3 CrB, HR 5747, HIP 75695, WDS 15278+2906) is a prototype of the peculiar A stars along with γ Equulei and α^2 CVn. Given the increased frequency with which planets seem to occur around higher mass stars (Johnson et al. 2007) and those showing higher metallicities (Gonzalez 1997; Santos et al. 2004; Fischer & Valenti 2005), this is a particularly compelling target. Furthermore, Neubauer (1944) identified a second period of nearly a year ($P_2 \sim 320$ days) in radial velocity observations. Kamper et al. (1990) presented new data that were inconsistent with the proposed perturbation, suggesting the orbital inclination had rotated to be face-on since the first half of that century. The calculations based on Holman & Wiegert (1999) predict such a companion would not have a stable orbit. Finally Söderhjelm

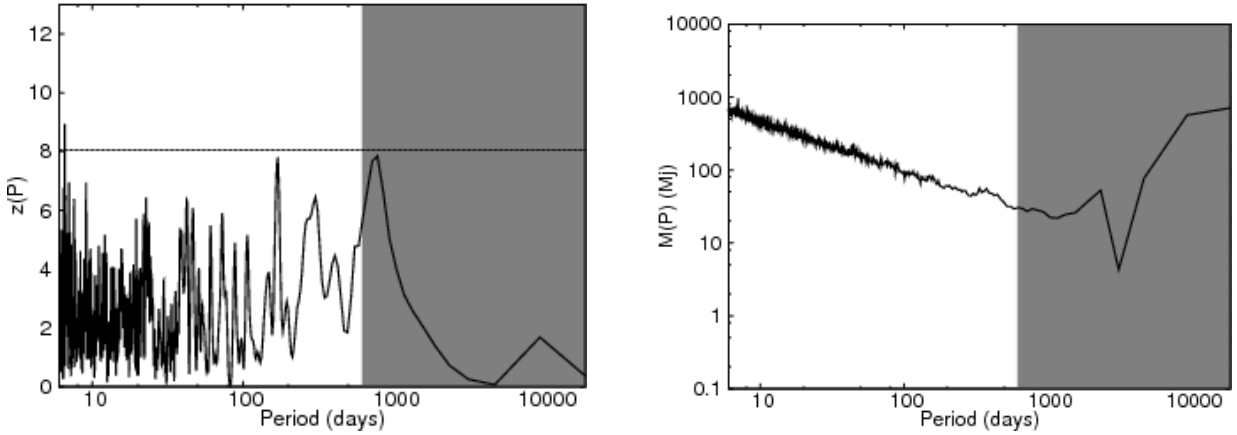


Figure 8. z -periodogram (left) and the mass-period companion phase space for HD 77327 (right). Companions in the regions above the plotted exclusion curve with circular orbits with any orientation are not consistent with the PHASES observations, with 99% confidence. Companions as small as 29 Jupiter masses in stable orbits can be ruled out by PHASES observations.

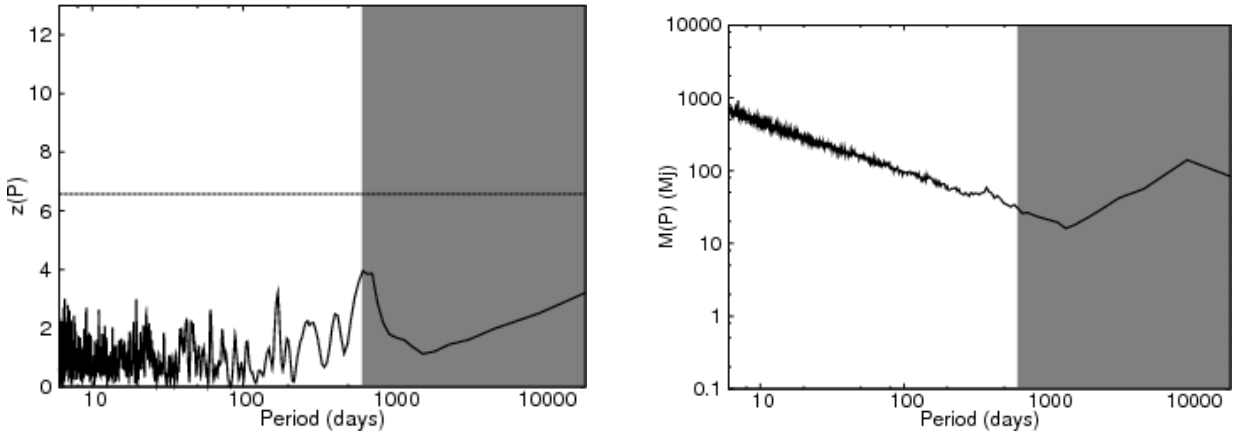


Figure 9. z -periodogram (left) and the mass-period companion phase space for HD 77327 (right). Companions in the regions above the plotted exclusion curve with circular orbits with any orientation are not consistent with the PHASES observations, with 99% confidence. Companions as small as 32 Jupiter masses in stable orbits can be ruled out by the combined observations.

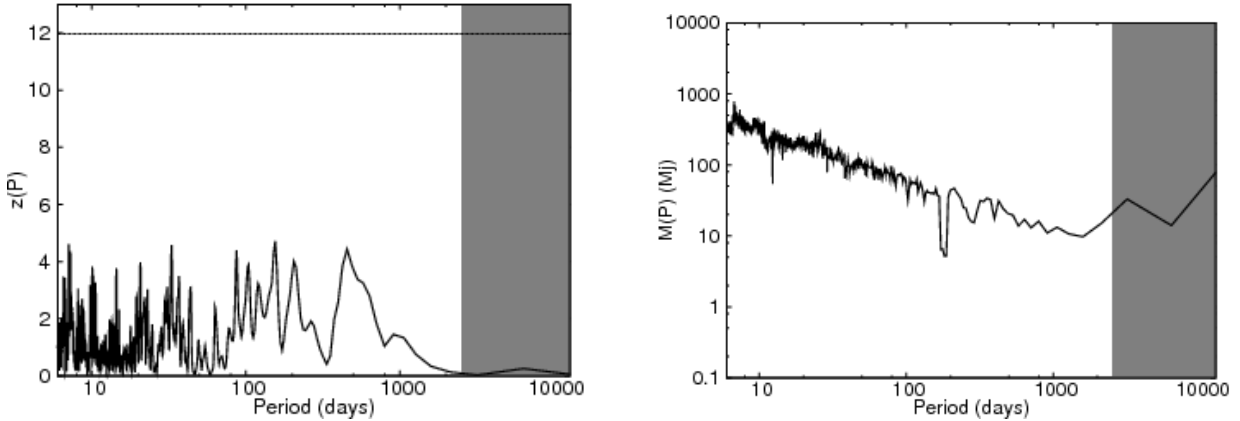


Figure 10. z -periodogram (left) and the mass-period companion phase space for HD 81858 (right). Companions in the regions above the plotted exclusion curve with circular orbits with any orientation are not consistent with the PHASES observations, with 99% confidence. Companions as small as 5.2 Jupiter masses can be ruled out by PHASES observations.

(1999) used *Hipparcos* astrometry to show no such companion could exist, a result verified by early PHASES results (Muterspaugh et al. 2006b).

With the full PHASES data set being analyzed using the revised approach described in this paper, the FAP of the highest peak ($z = 4.55$ at $P = 6.07$ days) in the z -periodogram is 53.9% with 99% detection confidence

requiring $z = 7.94$. The periodogram and companion mass limits are plotted in Figure 15.

3.14. HD 140159

HD 140159 (ι Ser, 21 Set, HR 5842, HIP 76852, WDS 15416+1940) is a pair of early A dwarfs. Being relatively massive stars a fairly large distance away, limits can only

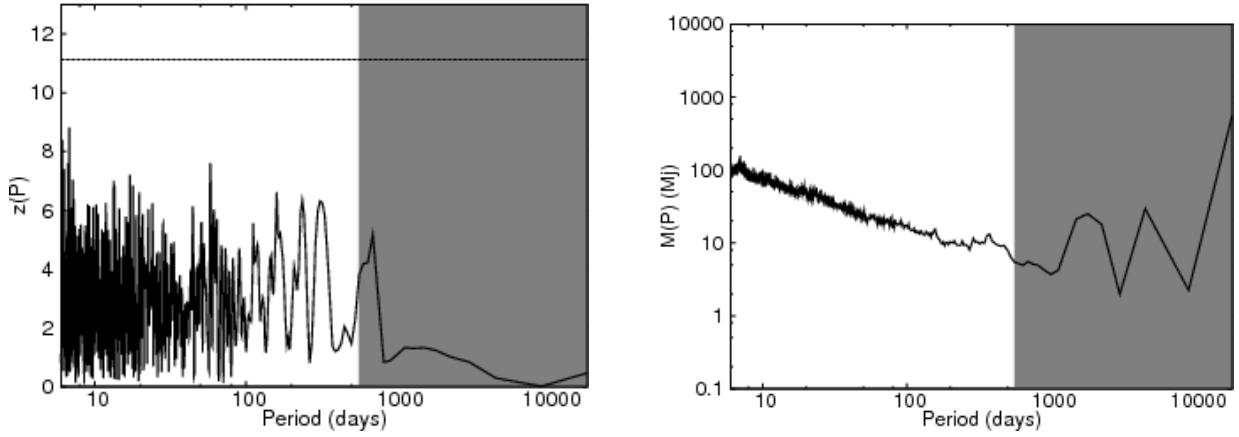


Figure 11. z -periodogram (left) and the mass-period companion phase space for HD 114378 (right). Companions in the regions above the plotted exclusion curve with circular orbits with any orientation are not consistent with the PHASES observations, with 99% confidence. Companions as small as 6.3 Jupiter masses can be ruled out by PHASES observations.

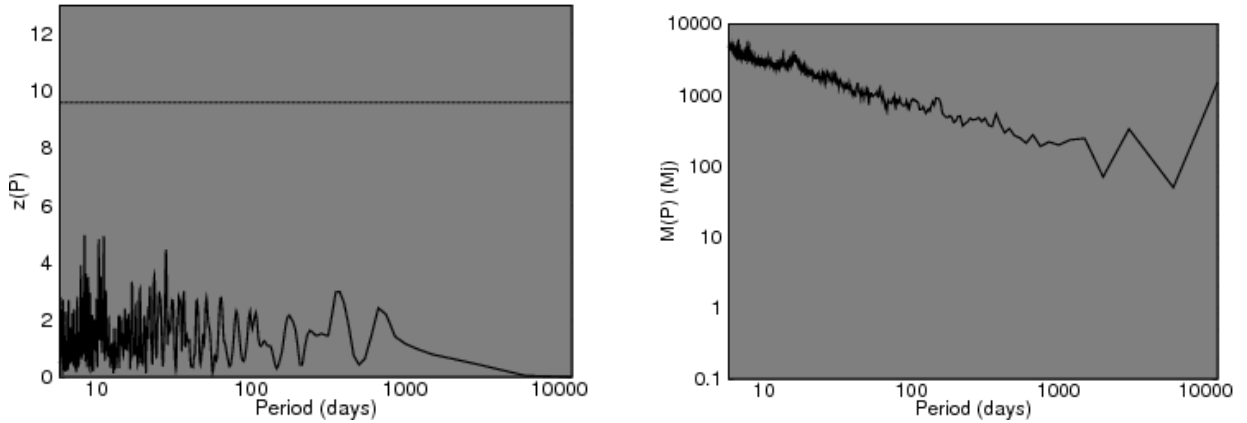


Figure 12. z -periodogram (left) and the mass-period companion phase space for HD 129246 (right). Companions in the regions above the plotted exclusion curve with circular orbits with any orientation are not consistent with the PHASES observations, with 99% confidence.

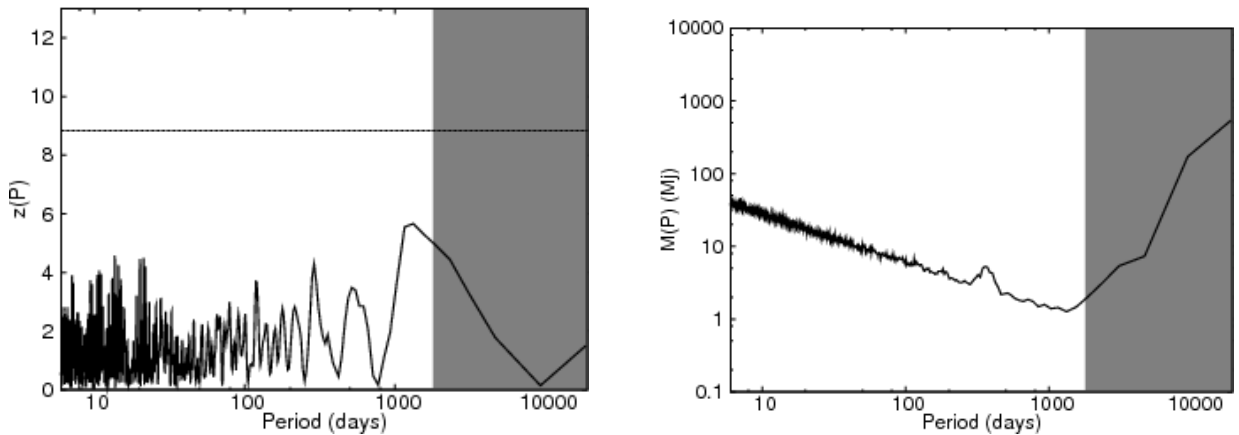


Figure 13. z -periodogram (left) and the mass-period companion phase space for HD 137107 (right). Companions in the regions above the plotted exclusion curve with circular orbits with any orientation are not consistent with the PHASES observations, with 99% confidence. Companions as small as 1.3 Jupiter masses can be ruled out by PHASES observations.

be placed on the existence of tertiary companions with masses in the brown dwarf or larger regime. The FAP of the highest peak ($z = 5.74$ at $P = 6.72$ days) in the z -periodogram is 36.1% with 99% detection confidence requiring $z = 12.65$. The periodogram and companion mass limits are plotted in Figure 16.

3.15. HD 140436

Like HD 140159, HD 140436 (γ CrB, 8 Crb, HR 5849, HIP 76952, WDS 15427+2618) is a pair of early A stars. Both its binarity and early spectral type limit its ability to be studied by the radial velocity method for exoplanet searches, highlighting another manner in which astrometry can complement other techniques. Objects as small

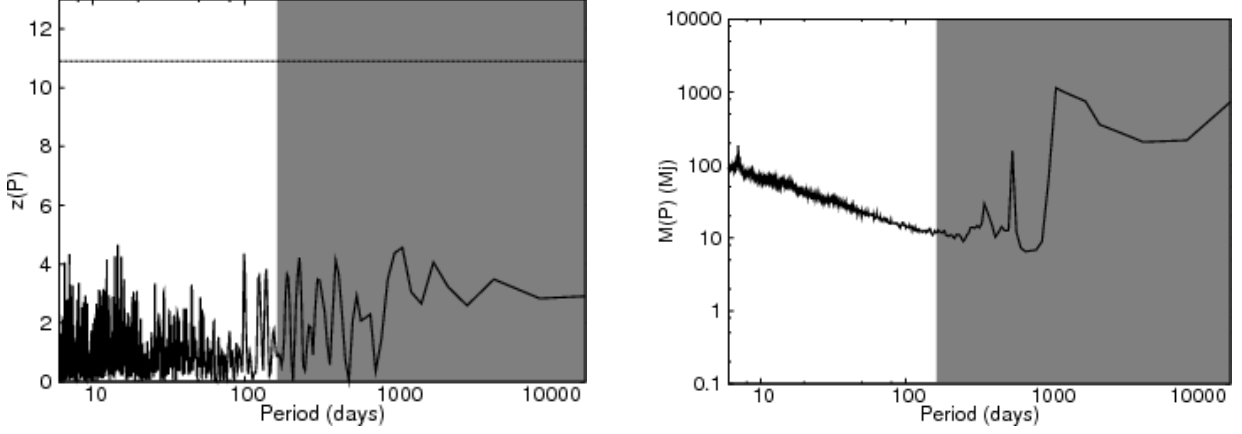


Figure 14. z -periodogram (left) and the mass-period companion phase space for HD 137391 (right). Companions in the regions above the plotted exclusion curve with circular orbits with any orientation are not consistent with the PHASES observations, with 99% confidence. Companions as small as 11 Jupiter masses can be ruled out by PHASES observations.

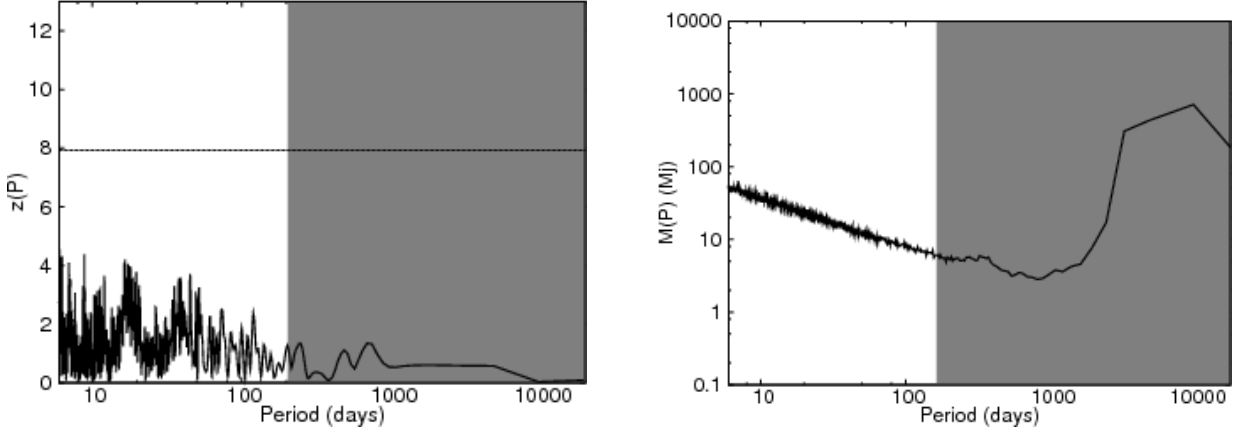


Figure 15. z -periodogram (left) and the mass-period companion phase space for HD 137909 (right). Companions in the regions above the plotted exclusion curve with circular orbits with any orientation are not consistent with the PHASES observations, with 99% confidence. Companions as small as 4.8 Jupiter masses in stable orbits can be ruled out by PHASES observations.

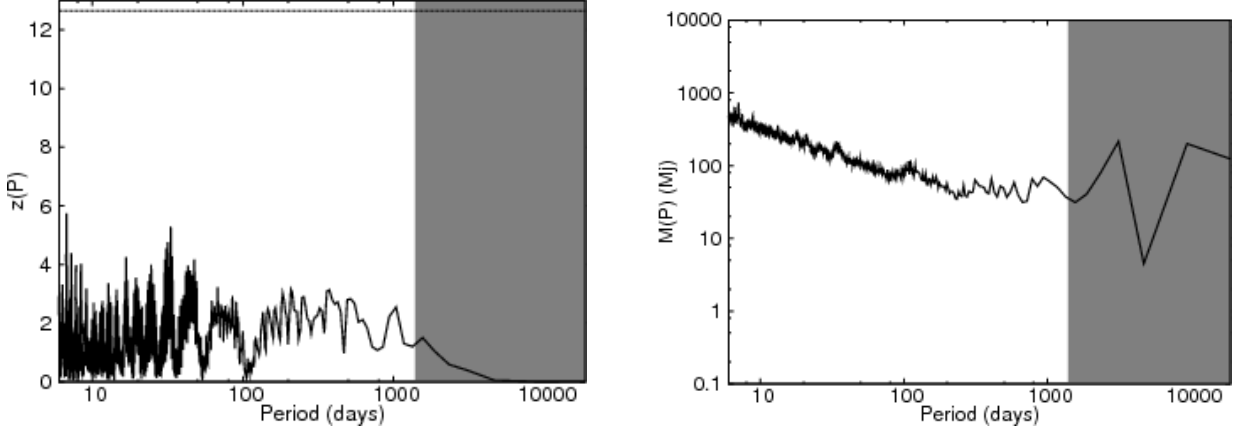


Figure 16. z -periodogram (left) and the mass-period companion phase space for HD 140159 (right). Companions in the regions above the plotted exclusion curve with circular orbits with any orientation are not consistent with the PHASES observations, with 99% confidence. Companions as small as 31 Jupiter masses can be ruled out by PHASES observations.

as the largest of giant planets can be ruled out for some stable orbital periods in this system, despite the relatively large masses of the stars and distance to the system. Some lower mass objects could have been detected if in fortunate orbital configurations (face-on orbits, or aligned parallel to the interferometer baseline vector)—

as is the case for the other systems, the limits presented in Figure 17 consider all possible low-eccentricity orbits. The FAP of the highest peak ($z = 5.40$ at $P = 10.2$ days) in the z -periodogram is 23.8% with 99% detection confidence requiring $z = 8.26$.

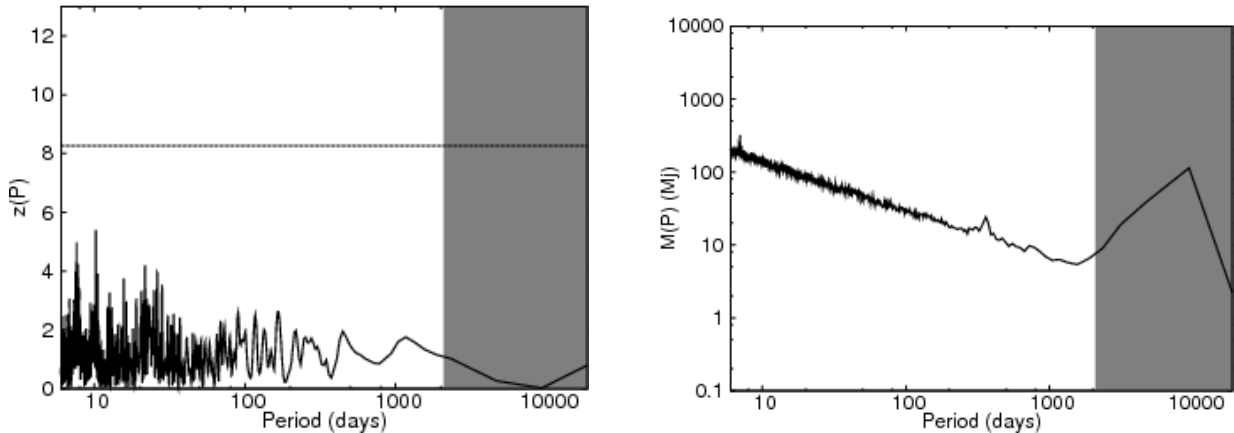


Figure 17. z -periodogram (left) and the mass-period companion phase space for HD 140436 (right). Companions in the regions above the plotted exclusion curve with circular orbits with any orientation are not consistent with the PHASES observations, with 99% confidence. Companions as small as 5.4 Jupiter masses can be ruled out by PHASES observations.

3.16. HD 155103

With only 10 PHASES measurements spanning just over two years, observing cadence causes more significant problems for HD 155103 (c Her, HR 6377, HIP 83838, WDS 17080+3556) than most of the other binaries. The cadence results in multiple spikes in the mass-period sensitivity plot corresponding to orbital periods when orbit aliasing is more likely. Combined with the relatively large mass of the components ($1.66 M_{\odot}$) and distance to the system (~ 56 pc), only limited constraints can be placed on tertiary companions. The FAP of the highest peak ($z = 8.03$ at $P = 7.36$ days) in the z -periodogram is 41.5%, whereas 99% confidence of detection would have only occurred for values larger than $z = 32.0$. The periodogram and companion mass limits are plotted in Figure 18.

3.17. HD 187362

Like HD 155103, only 10 PHASES measurements of HD 187362 (ζ Sge, 8 Sge, HR 7546, HIP 97496, WDS 19490+1909) were made, though in this case with an even shorter timespan of 1.2 yr. These relatively faint systems could not be observed until the instrument improvements were made that allowed the slower 20 Hz fringe tracking. It too is relatively massive (average stellar mass $2.35 M_{\odot}$) and yet more distant (~ 100 pc) and only stellar mass objects in stable orbits can be excluded. Also like HD 155103, the detection limit graph shows a jagged transition between the regions in which companions can and cannot be ruled out, due to observing cadence. The FAP of the highest peak ($z = 2.32$ at $P = 18.1$ days) in the z -periodogram is 90.9%, with 1% FAP requiring $z = 18.7$. The periodogram and companion mass limits are plotted in Figure 19.

3.18. HD 202275

HD 202275 (δ Equ, 7 Equ, HR 8123, HIP 104858, WDS 21145+1000) was studied extensively by PHASES (Mutterspaugh et al. 2006a, 2008), with a span of observations of 1866 days, covering nearly the full binary orbit (2084 days). Companions as small as 3.8 Jupiter masses can be ruled out in stable orbits having any orientation. The FAP of the highest peak ($z = 6.20$ at $P = 509$ days) in the z -periodogram is 9.4%, with 1% FAP requiring

$z = 7.86$. The periodogram and companion mass limits are plotted in Figure 20.

3.19. HD 202444

There is some indication that τ Cyg may have a substellar companion orbiting one of the two stars (see Paper V). There are reasons to doubt the authenticity of this proposed companion, so the visual orbit obtained by modeling the system with only a single Keplerian model has been presented in Paper II in addition to the double Keplerian model presented in Paper V. If real, the companion has a long orbital period. When only the shorter timespan PHASES data were analyzed to search for tertiary companions, the signal was absorbed into that of the wider binary, so no compelling evidence for a companion was present. However, the continued large value of χ^2 that resulted when the combined PHASES and non-PHASES astrometry set was analyzed prompted a second search for tertiary companions, this time using all the astrometric measurements. The longer timespan non-PHASES astrometry measurements better constrained the binary orbit parameters, preventing them from taking incorrect values to absorb the motion caused by an intermediate period companion (shorter than the binary motion, but long compared to the timespan of PHASES measurements) and indicated the presence of a companion with mass corresponding to that of a giant planet.

Because the companion only presents itself when both PHASES and non-PHASES measurements are jointly analyzed, it is more uncertain that the object is real. This contrasts with the other candidate objects listed in Paper V, which could be detected both when just the PHASES measurements were considered and in the combined analysis. For this reason, HD 202444 has been included in the present analysis to demonstrate what other companions can be shown not to exist in the case that the detected companion is not real either.

For the PHASES-only analysis, the FAP of the highest peak ($z = 5.93$ at $P = 25.5$ days) in the z -periodogram is 19.1%, with 1% FAP requiring $z = 8.92$. However, when PHASES measurements are analyzed along with non-PHASES astrometry covering more of the binary orbit, the highest peak in the z -periodogram is $z = 51.9$ at $P = 826$ days with an FAP of 0.0%. This peak is above

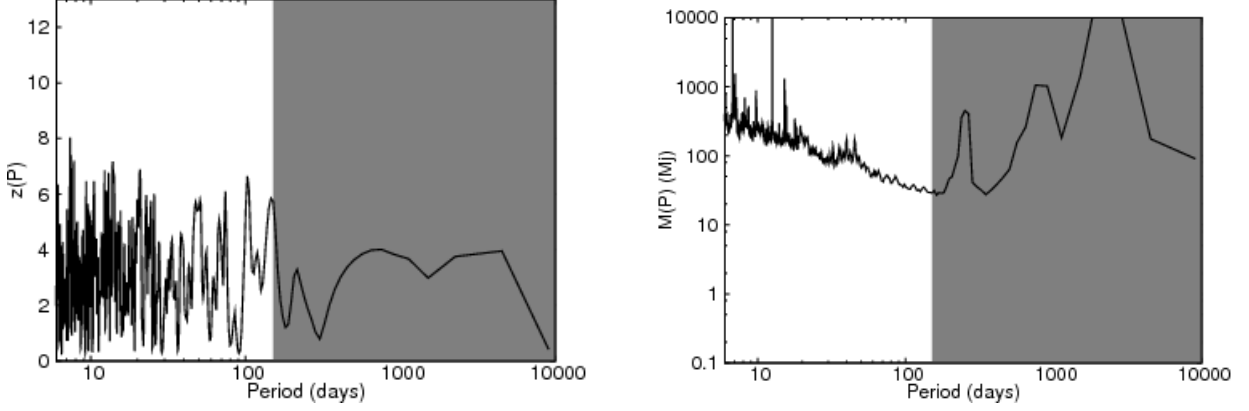


Figure 18. z -periodogram (left) and the mass-period companion phase space for HD 155103 (right). Companions in the regions above the plotted exclusion curve with circular orbits with any orientation are not consistent with the PHASES observations, with 99% confidence. Companions as small as 29 Jupiter masses can be ruled out by PHASES observations.

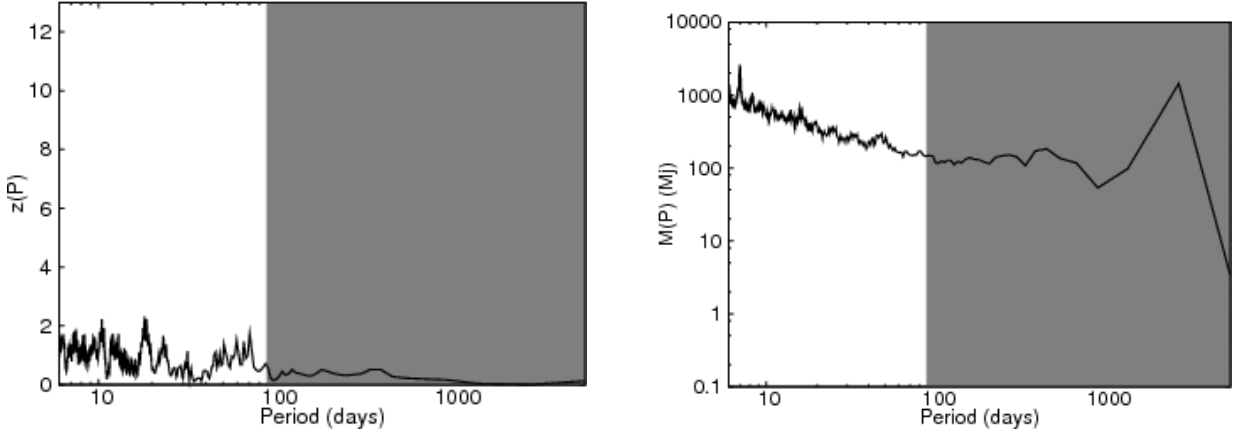


Figure 19. z -periodogram (left) and the mass-period companion phase space for HD 187362 (right). Companions in the regions above the plotted exclusion curve with circular orbits with any orientation are not consistent with the PHASES observations, with 99% confidence. Companions as small as 142 Jupiter masses can be ruled out by PHASES observations, roughly twice as massive as the largest of brown dwarfs.

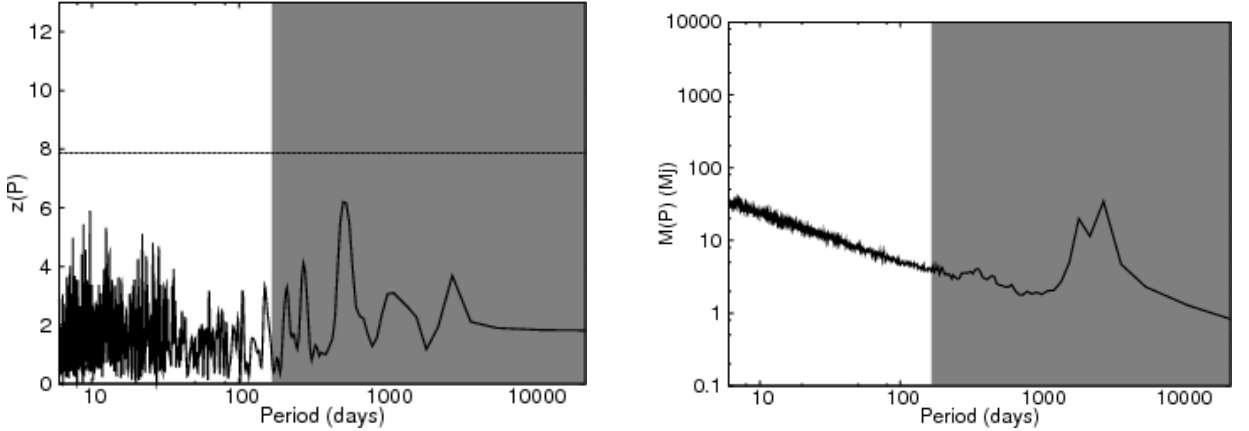


Figure 20. z -periodogram (left) and the mass-period companion phase space for HD 202275 (right). Companions in the regions above the plotted exclusion curve with circular orbits with any orientation are not consistent with the PHASES observations, with 99% confidence. Companions as small as 3.8 Jupiter masses in stable orbits can be ruled out by PHASES observations.

the 1% FAP mark, which would be at $z = 10.1$. The periodogram and companion mass limits when only PHASES observations are analyzed are plotted in Figure 21 and those for the combined data set are plotted in Figure 22, assuming the companion object is not real.

3.20. HD 207652

The periodogram and mass-period limits for HD 207652 (13 Peg, HR 8344, HIP 107788, V373 Peg, WDS 21501+1717) are plotted in Figure 23. The FAP of the highest peak ($z = 5.19$ at $P = 15.8$ days) in the z -periodogram is 29.9% with 99% detection confidence re-

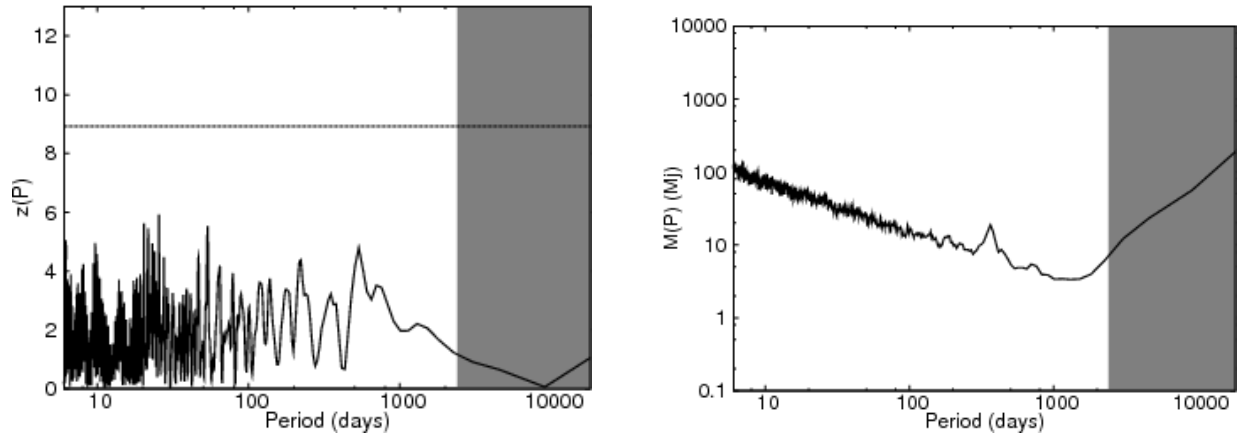


Figure 21. z -periodogram (left) and the mass-period companion phase space for HD 202444 (right), assuming that the candidate object is not real. Companions in the regions above the plotted exclusion curve with circular orbits with any orientation are not consistent with the PHASES observations, with 99% confidence. Companions as small as 3.3 Jupiter masses in stable orbits can be ruled out by PHASES observations.

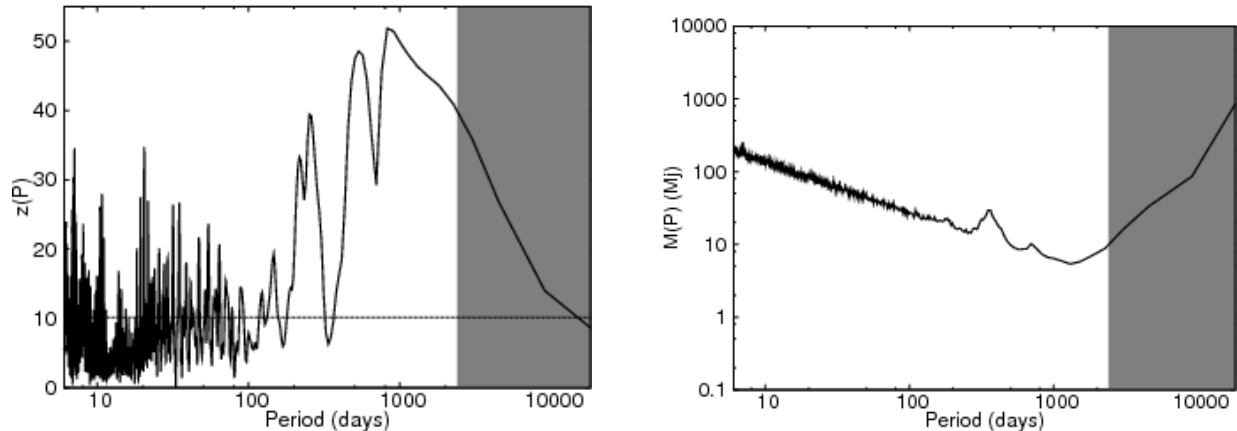


Figure 22. z -periodogram (left) and the mass-period companion phase space for HD 202444 (right), assuming that the candidate object is not real. Companions in the regions above the plotted exclusion curve with circular orbits with any orientation are not consistent with the PHASES observations, with 99% confidence. Companions as small as 5.4 Jupiter masses in stable orbits can be ruled out by the combined observations.

quiring $z = 7.78$. With a relatively large range of orbital periods that can be stable (up to 3.3 yr) and number of PHASES measurements (51), there is increased sensitivity to companion objects in HD 207652 than most of the other systems being considered. Companions as small as 2.2 Jupiter masses can be ruled out in this binary. It is worth noting that Tamazian et al. (1999) claim the secondary in the system is a T Tauri star, so this represents a possible non-detection of planets in a forming system.

3.21. HD 214850

In the analysis of just the PHASES observations of HD 214850 (HR 8631, HIP 111974, WDS 22409+1433), the FAP of the highest peak ($z = 7.08$ at $P = 14.4$ days) in the z -periodogram is 3.8%. The peak value $z = 7.08$ is close to the 1% FAP limit at $z = 7.78$. As were the cases for HD 26690 and HD 77327, this low value inspired a second search including non-PHASES data from the WDS, as listed in Paper II. This revised search found a peak of $z = 5.63$ at $P = 15.9$ days with an FAP of 9.5% and well below $z = 7.06$ which would correspond to 1% FAP. Because the identified orbital period is different and the combined FAP is well beyond the 1% threshold, there is not sufficient evidence to claim the existence of

a companion object in this system. The z -periodograms and mass-period phase space plots for the analysis of HD 214850 are shown in Figures 24 and 25.

4. FUTURE DIRECTIONS

The PHASES program used the same interferometric astrometry concepts as will be used in the SIM-Lite Astrometric Observatory mission (Shao et al. 1995; Unwin et al. 2008). SIM-Lite will benefit from greater stability and sensitivity that operating in a space environment allows, introducing improved measurement precisions and versatility. SIM-Lite astrometry operating on single stars can achieve measurement precisions over 1.5 orders of magnitude better than those presented here, with $10\text{-}100\times \sim 30$ more measurements, on a much more flexible set of targets, including stars $\sim 10\times$ closer to the solar system. Overall, this means a factor of $35 \times \sqrt{30} \times 10 \sim 2000$ better sensitivity to companions. In addition, those measurements will be more two-dimensional than PHASES since the baseline will be rotated to two fully orthogonal directions. SIM-Lite will move from the ~ 10 (typical) and ~ 1 (best) Jupiter-mass sensitivities of the present study into the regime of Earthlike planets.

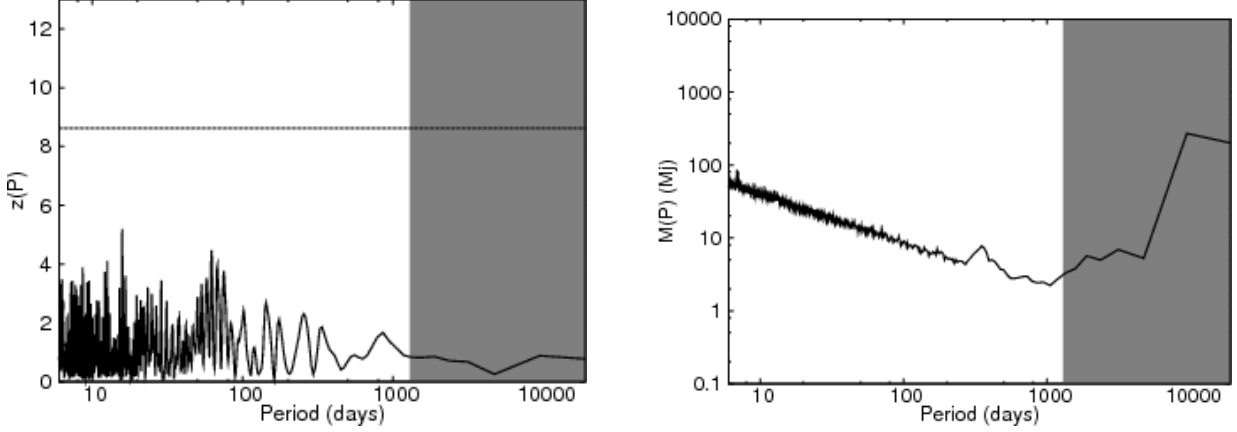


Figure 23. z -periodogram (left) and the mass-period companion phase space for HD 207652 (right). Companions in the regions above the plotted exclusion curve with circular orbits with any orientation are not consistent with the PHASES observations, with 99% confidence. Companions as small as 2.2 Jupiter masses can be ruled out by PHASES observations.

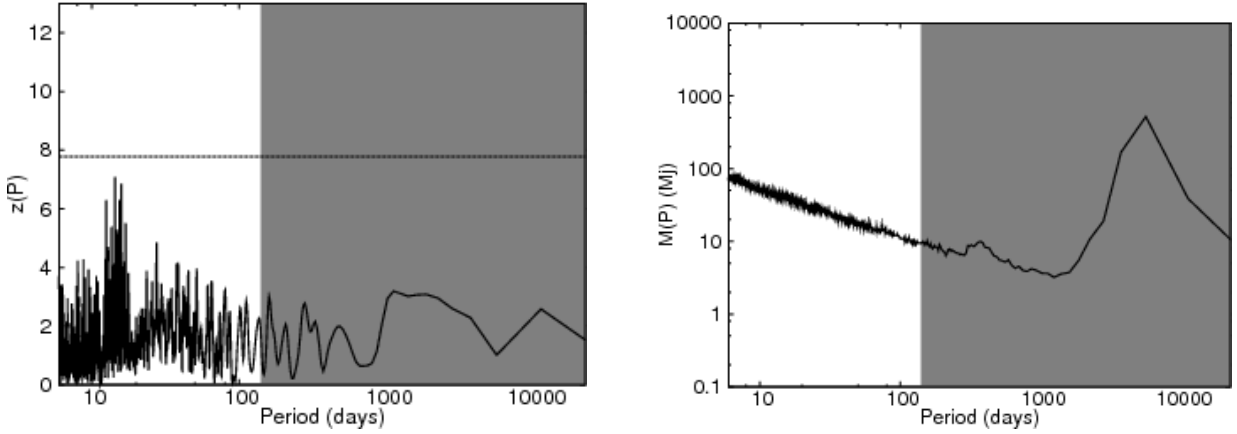


Figure 24. z -periodogram (left) and the mass-period companion phase space for HD 214850 (right). Companions in the regions above the plotted exclusion curve with circular orbits with any orientation are not consistent with the PHASES observations, with 99% confidence. Companions as small as 8.8 Jupiter masses in stable orbits can be ruled out by PHASES observations.

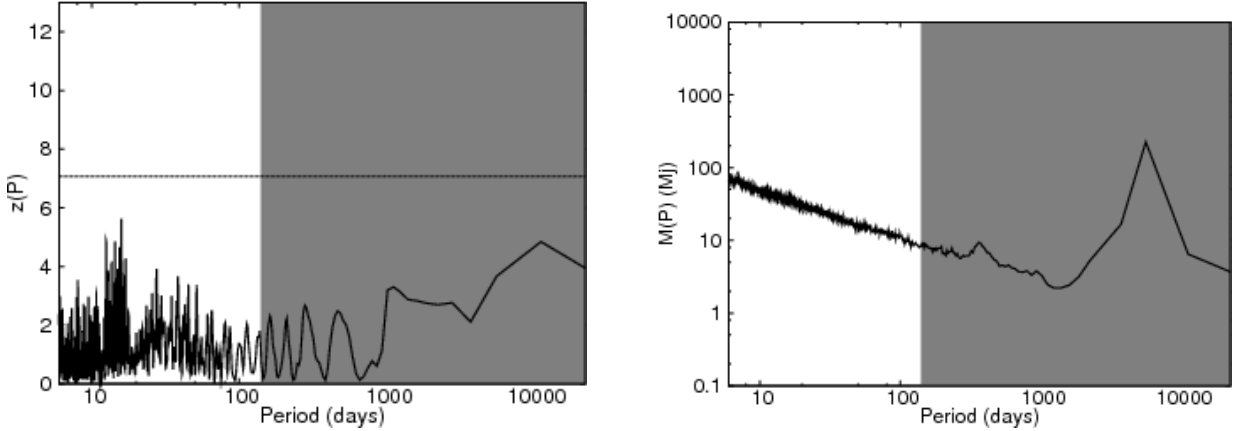


Figure 25. z -periodogram (left) and the mass-period companion phase space for HD 214850 (right). Companions in the regions above the plotted exclusion curve with circular orbits with any orientation are not consistent with the PHASES observations, with 99% confidence. Companions as small as 8.3 Jupiter masses in stable orbits can be ruled out by the combined observations.

PHASES benefits from the efforts of the PTI collaboration members who have each contributed to the development of an extremely reliable observational instrument. Without this outstanding engineering effort to produce a solid foundation, advanced phase-referencing techniques would not have been possible. We thank

PTI's night assistant Kevin Rykoski for his efforts to maintain PTI in excellent condition and operating PTI in phase-referencing mode every week. Part of the work described in this paper was performed at the Jet Propulsion Laboratory under contract with the National Aeronautics and Space Administration. Interferometer data were

obtained at the Palomar Observatory with the NASA Palomar Testbed Interferometer, supported by NASA contracts to the Jet Propulsion Laboratory. This publication makes use of data products from the Two Micron All Sky Survey, which is a joint project of the University of Massachusetts and the Infrared Processing and Analysis Center/California Institute of Technology, funded by the National Aeronautics and Space Administration and the National Science Foundation. This research has made use of the Simbad database, operated at CDS, Strasbourg, France. M.W.M. acknowledges support from the Townes Fellowship Program, Tennessee State University, and the state of Tennessee through its Centers of Excellence program. Some of the software used for analysis was developed as part of the SIM Double Blind Test with support from NASA contract NAS7-03001 (JPL 1336910). PHASES is funded in part by the California Institute of Technology Astronomy Department, and by the National Aeronautics and Space Administration under grant no. NNG05GJ58G issued through the Terrestrial Planet Finder Foundation Science Program. This work was supported in part by the National Science Foundation through grants AST 0300096, AST 0507590, and AST 0505366. M.K. is supported by the Foundation for Polish Science through a FOCUS grant and fellowship, by the Polish Ministry of Science and Higher Education through grant N203 3020 35.

Facilities: PO:PTI

REFERENCES

- Abt, H. A. & Levy, S. G. 1976, *ApJS*, 30, 273
- Bevington, P. R. & Robinson, D. K. 2003, *Data reduction and error analysis for the physical sciences*, ed. Bevington, P. R. & Robinson, D. K.
- Boss, A. P. 1998, *Bulletin of the American Astronomical Society*, 30, 1048
- Campbell, B., Walker, G. A. H., & Yang, S. 1988, *ApJ*, 331, 902
- Colavita, M. M., Wallace, J. K., Hines, B. E., Gursel, Y., Malbet, F., Palmer, D. L., Pan, X. P., Shao, M., Yu, J. W., Boden, A. F., Dumont, P. J., Gubler, J., Koresko, C. D., Kulkarni, S. R., Lane, B. F., Mobley, D. W., & van Belle, G. T. 1999, *ApJ*, 510, 505
- Correia, A. C. M., Lagrange, A., Udry, S., Fusco, T., Galland, F., Naef, D., Beuzit, J., & Mayor, M. 2006, *A&A* in press, <http://arxiv.org/abs/astro-ph/0606166>
- Cumming, A., Marcy, G. W., & Butler, R. P. 1999, *ApJ*, 526, 890
- Desidera, S. & Barbieri, M. 2007, *A&A*, 462, 345
- Duquenois, A. & Mayor, M. 1991, *A&A*, 248, 485
- Dvorak, R. 1982, *Oesterreichische Akademie Wissenschaften Mathematisch naturwissenschaftliche Klasse Sitzungsberichte Abteilung*, 191, 423
- Eggenberger, A., Udry, S., Mazeh, T., Segal, Y., & Mayor, M. 2007, *A&A*, 466, 1179
- Fischer, D. A. & Valenti, J. 2005, *ApJ*, 622, 1102
- Gonzalez, G. 1997, *MNRAS*, 285, 403
- Griffin, R. F. 1999, *The Observatory*, 119, 272
- Hatzes, A. P., Cochran, W. D., Endl, M., McArthur, B., Paulson, D. B., Walker, G. A. H., Campbell, B., & Yang, S. 2003, *ApJ*, 599, 1383
- Hatzes, A. P. & Wuchterl, G. 2005, *Nature*, 436, 182
- Holman, M. J. & Wiegert, P. A. 1999, *AJ*, 117, 621
- Howard, A. W., Johnson, J. A., Marcy, G. W., Fischer, D. A., Wright, J. T., Bernat, D., Henry, G. W., Peek, K. M. G., Isaacson, H., Apps, K., Endl, M., Cochran, W. D., Valenti, J. A., Anderson, J., & Piskunov, N. E. 2010, *ApJ*, 721, 1467
- Johnson, J. A., Butler, R. P., Marcy, G. W., Fischer, D. A., Vogt, S. S., Wright, J. T., & Peek, K. M. G. 2007, *ApJ*, 670, 833
- Kamper, K. W., McAlister, H. A., & Hartkopf, W. I. 1990, *AJ*, 100, 239
- Kirkpatrick, J. D., Dahn, C. C., Monet, D. G., Reid, I. N., Gizis, J. E., Liebert, J., & Burgasser, A. J. 2001, *AJ*, 121, 3235
- Konacki, M. 2005, *Nature*, 436, 230
- Lagrange, A., Beust, H., Udry, S., Chauvin, G., & Mayor, M. 2006, *A&A*, in press, [astro-ph/0606167](http://arxiv.org/abs/astro-ph/0606167)
- Lane, B. F. & Muterspaugh, M. W. 2004, *ApJ*, 601, 1129
- Marzari, F. & Scholl, H. 2000, *ApJ*, 543, 328
- Marzari, F., Thebault, P., Kortenamp, S., & Scholl, H. 2007, *ArXiv e-prints*, 705
- Mason, B. D., Wycoff, G. L., Hartkopf, W. I., Douglass, G. G., & Worley, C. E. 2001, *AJ*, 122, 3466
- , 2010, <http://www.usno.navy.mil/USNO/astrometry/optical-IR-prod/wds/WDS>
- Mazeh, T., Tsodikovich, Y., Segal, Y., Zucker, S., Eggenberger, A., Udry, S., & Mayor, M. 2009, *MNRAS*, 399, 906
- Morbey, C. L. & Griffin, R. F. 1987, *ApJ*, 317, 343
- Mugrauer, M. & Neuhäuser, R. 2005, *MNRAS*, 361, L15
- Muterspaugh, M. W., Fekel, F. C., Lane, B. F., Hartkopf, W. I., Kulkarni, S. R., Konacki, M., Burke, B. F., Colavita, M. M., Shao, M., & Williamson, M. 2010a, Submitted to *AJ*
- Muterspaugh, M. W., Hartkopf, W. I., Lane, B. F., O’Connell, J., Williamson, M., Kulkarni, S. R., Konacki, M., Burke, B. F., Colavita, M. M., Shao, M., & Wiktorowicz, S. J. 2010b, Submitted to *AJ*
- Muterspaugh, M. W., Lane, B. F., Fekel, F. C., Konacki, M., Burke, B. F., Kulkarni, S. R., Colavita, M. M., Shao, M., & Wiktorowicz, S. J. 2008, *AJ*, 135, 766
- Muterspaugh, M. W., Lane, B. F., Konacki, M., Wiktorowicz, S., Burke, B. F., Colavita, M. M., Kulkarni, S. R., & Shao, M. 2006a, *ApJ*, 636, 1020
- Muterspaugh, M. W., Lane, B. F., Kulkarni, S. R., Burke, B. F., Colavita, M. M., & Shao, M. 2006b, *ApJ*, 653, 1469
- Muterspaugh, M. W., Lane, B. F., Kulkarni, S. R., Konacki, M., Burke, B. F., Colavita, M. M., Shao, M., Hartkopf, W. I., Boss, A. P., & Williamson, M. 2010c, Submitted to *AJ*
- Muterspaugh, M. W., Lane, B. F., Kulkarni, S. R., Konacki, M., Burke, B. F., Colavita, M. M., Shao, M., Wiktorowicz, S. J., & O’Connell, J. 2010d, Submitted to *AJ*
- Neubauer, F. J. 1944, *ApJ*, 99, 134
- Pfahl, E. 2005, *ApJ*, 635, L89
- Pfahl, E. & Muterspaugh, M. 2006, *ApJ*, 652, 1694
- Pichardo, B., Sparke, L. S., & Aguilar, L. A. 2005, *MNRAS*, 359, 521
- Queloz, D., Mayor, M., Weber, L., Blécha, A., Burnet, M., Confino, B., Naef, D., Pepe, F., Santos, N., & Udry, S. 2000, *A&A*, 354, 99
- Raghavan, D., Henry, T. J., Mason, B. D., Subasavage, J. P., Jao, W., Beaulieu, T. D., & Hambly, N. C. 2006, *ApJ*, 646, 523
- Santos, N. C., Israelian, G., & Mayor, M. 2004, *A&A*, 415, 1153
- Scarfe, C. D. & Fekel, F. C. 1978, *PASP*, 90, 297
- Shao, M., Livermore, T. R., Wolff, D. M., Yu, J. W., & Colavita, M. M. 1995, *Bulletin of the American Astronomical Society*, 27, 1384
- Simon, M., Ghez, A. M., Leinert, C., Cassar, L., Chen, W. P., Howell, R. R., Jameson, R. F., Matthews, K., Neugebauer, G., & Richichi, A. 1995, *ApJ*, 443, 625
- Söderhjelm, S. 1999, *A&A*, 341, 121
- Tamazian, V. S., Docobo, J. A., & Melikian, N. D. 1999, *ApJ*, 513, 933
- Thébault, P., Marzari, F., Scholl, H., Turrini, D., & Barbieri, M. 2004, *A&A*, 427, 1097
- Traub, W. A., Beichman, C., Boden, A. F., Boss, A. P., Casertano, S., Catanzarite, J., Fischer, D., Ford, E. B., Gould, A., Halverson, S., Howard, A., Ida, S., Kasdin, N. J., Laughlin, G. P., Levison, H. F., Lin, D., Makarov, V., Marr, J., Muterspaugh, M., Raymond, S. N., Savransky, D., Shao, M., Sozzetti, A., & Zhai, C. 2010, in *EAS Publications Series*, Vol. 42, *EAS Publications Series*, ed. K. Goździewski, A. Niedzielski, & J. Schneider, 191–199
- Traub, W. A., Ford, E., Laughlin, G., Levison, H., Lin, D., Raymond, S., Makarov, V., Casertano, S., Fischer, D., Kasdin, J., Muterspaugh, M., Shao, M., Beichman, C., Boss, A., Gould, A., & Marr, J. 2009, in *Bulletin of the American Astronomical Society*, Vol. 41, *Bulletin of the American Astronomical Society*, 267–+

- Unwin, S. C., Shao, M., Tanner, A. M., Allen, R. J., Beichman, C. A., Boboltz, D., Catanzarite, J. H., Chaboyer, B. C., Ciardi, D. R., Edberg, S. J., Fey, A. L., Fischer, D. A., Gelino, C. R., Gould, A. P., Grillmair, C., Henry, T. J., Johnston, K. V., Johnston, K. J., Jones, D. L., Kulkarni, S. R., Law, N. M., Majewski, S. R., Makarov, V. V., Marcy, G. W., Meier, D. L., Olling, R. P., Pan, X., Patterson, R. J., Pitesky, J. E., Quirrenbach, A., Shaklan, S. B., Shaya, E. J., Strigari, L. E., Tomsick, J. A., Wehrle, A. E., & Worthey, G. 2008, *PASP*, 120, 38
- Wright, J. T. & Howard, A. W. 2009, *ApJS*, 182, 205
- Zucker, S., Mazeh, T., Santos, N. C., Udry, S., & Mayor, M. 2004, *A&A*, 426, 695